Development 127, 2433-2445 (2000)
Printed in Great Britain © The Company of Biologists Limited 2000
DEV4341

The homeobox gene *Hex* is required in definitive endodermal tissues for normal forebrain, liver and thyroid formation

Juan Pedro Martinez Barbera[1,*], Melanie Clements[1,*], Paul Thomas[2], Tristan Rodriguez[1], Denise Meloy[1], Dimitris Kioussis[3] and Rosa S. P. Beddington[1,‡]

[1]Division of Mammalian Development, National Institute for Medical Research, The Ridgeway, London, NW7 1AA, UK
[2]Gene Discovery Unit, The Murdoch Institute, Royal Children's Hospital, Parkville, Victoria 3052, AUSTRALIA
[3]Division of Molecular Immunology, National Institute for Medical Research, The Ridgeway, London, NW7 1AA, UK
*J. P. M. B. and M. C. contributed equally to this work
‡Author for correspondence (e-mail: rbeddin@nimr.mrc.ac.uk)

Accepted 17 March; published on WWW 10 May 2000

SUMMARY

The homeobox gene *Hex* is expressed in the anterior visceral endoderm (AVE) and rostral definitive endoderm of early mouse embryos. Later, *Hex* transcripts are detected in liver, thyroid and endothelial precursor cells. A null mutation was introduced into the *Hex* locus by homologous recombination in embryonic stem cells. *Hex* mutant embryos exhibit varying degrees of anterior truncation as well as liver and thyroid dysplasia. The liver diverticulum is formed but migration of hepatocytes into the septum transversum fails to occur. Development of the thyroid is arrested at the thyroid bud stage at 9.5 dpc. Brain defects are restricted to the rostral forebrain and have a caudal limit at the zona limitans intrathalamica, the boundary between dorsal and ventral thalamus. Analysis of *Hex*$^{-/-}$ mutants at early stages shows that the prospective forebrain ectoderm is correctly induced and patterned at 7.5 days post coitum (dpc), but subsequently fails to develop. AVE markers are expressed and correctly positioned but development of rostral definitive endoderm is greatly disturbed in *Hex*$^{-/-}$ embryos. Chimeric embryos composed of *Hex*$^{-/-}$ cells developing within a wild-type visceral endoderm show forebrain defects indicating that *Hex* is required in the definitive endoderm. All together, these results demonstrate that *Hex* function is essential in definitive endoderm for normal development of the forebrain, liver and thyroid gland.

Key words: Visceral endoderm, Definitive endoderm, Forebrain, Liver, Thyroid, Mouse

INTRODUCTION

Classical studies in amphibians have shown that a specific group of cells in the vertebrate gastrula, the organizer, is sufficient to induce a complete secondary axis when grafted into the ventral region of a host embryo (Spemann and Mangold, 1924). Transplantation of the mouse organizer (the node) has been conducted using donor tissue isolated from full-length and early-streak mouse embryos. Although, ectopic neural axes were obtained in both cases, the most anterior aspects of the neural axis were absent (Beddington, 1994; Tam and Steiner, 1999). These results suggest that the induction of the forebrain in the mouse embryo requires tissues not provided by the node.

In the mouse embryo there are two signalling centers required for normal brain formation: the anterior visceral endoderm (AVE) and the node and its derivatives. Genetic evidence for the role of the AVE in anterior patterning has been obtained from chimeric analysis where the epiblast is of one genotype and the primitive endoderm and trophectoderm lineages of another (see Beddington and Robertson, 1999). For example, chimeric analysis has shown that *Lim1* is required in the AVE to induce and initiate the patterning of the anterior neural plate (Shawlot et al., 1999). Likewise, *Hnf3β*, *Otx2* and *nodal* are required in the AVE for normal brain formation (Varlet et al., 1997; Dufort et al., 1998; Rhinn et al., 1998; Acampora et al., 1998). Grafting experiments in mouse have shown that the mouse AVE is unable to induce neural character in non-neural ectoderm. However, a graft containing a combination of the AVE, anterior epiblast and the early node is essential if a complete neural axis is to be induced (Tam and Steiner, 1999). Similarly, in embryos lacking *Wnt3* the early node is not formed but the AVE is correctly specified. This leads to an absence of *Hesx1* expression in the anterior neural plate, and a failure of *Otx2* expression to be restricted anteriorly (P. Liu et al., 1999). Moreover, both tissue recombination experiments and chimeric studies have shown that anterior axial mesendoderm tissue, derived from the node, is required for normal patterning of the rostral neural plate (Ang et al., 1994; Shawlot et al., 1999). These results suggest that in the mouse the AVE, the node and the axial mesendoderm cooperate in the induction and patterning of the brain.

The divergent homeobox gene *Hex* is expressed in the AVE

and definitive endoderm of the early mouse embryo, two tissues implicated in patterning the anterior neural plate (Crompton et al., 1992; Ang et al., 1994; Beddington and Robertson, 1999). Other domains of *Hex* expression are found in the liver, thyroid gland, lungs, endothelial cell precursors and multipotent hematopoietic cells (Crompton et al., 1992; Thomas et al., 1998; Keng et al., 1998). *Hex* orthologues have been cloned in human, *Xenopus*, chick and zebrafish (Bedford et al., 1993; Newman et al., 1997; Yatskievych et al., 1999; Ho et al., 1999). Grafting and overexpression experiments in *Xenopus* and zebrafish have suggested a role of *Hex* in formation of the vascular system and in embryonic anterior patterning (Newman et al., 1997; Jones et al., 1999). To define the function of *Hex* during mouse development, we have generated a targeted mutation in the *Hex* locus. $Hex^{-/-}$ embryos die at mid-gestation and show variable forebrain truncations, as well as liver and thyroid dysplasia. Therefore, *Hex* is needed in endodermal tissues for normal forebrain, liver and thyroid development.

MATERIALS AND METHODS

Targeting vector and generation of chimeras

The *Hex* genomic clone was isolated from a 129/Olac genomic library (gift from Dr Andrew Smith) using *Hex* cDNA as a probe (Thomas et al., 1998). To construct the targeting vector, 4.3 kb and 1.2 kb of 5′ and 3′ homologous regions were cloned on either side of an *IRES-lacZ-Neo* cassette (courtesy of Dr Andrew Smith; Fig. 1A). The *Hex* coding region from His^{5} to Asp^{199}, containing the entire homeodomain and a putative repressor domain in the N terminus, had been deleted (Crompton et al., 1992; Tanaka et al., 1999). This vector was linearised with *Pac*I and electroporated into E14 ES cells. After double selection with G418 and gancyclovir, 200 ES cell clones were picked, expanded and frozen according to standard methods (Hogan et al., 1994). To screen for homologous recombinants, ES cell DNA was digested with *Eco*RV and hybridised to sequences located 5′ (Fig. 1A) and 3′ external to the recombination sites. Ten correctly targeted clones were identified and three of them were used for injection into C57Bl6 blastocysts (Fig. 1B). Chimeric males from the three lines were mated with C57Bl6 females to establish F_1 heterozygotes. Results were pooled from the three heterozygous lines since they had identical phenotypes to $Hex^{-/-}$ embryos.

Genotyping of the wild-type and mutant *Hex* alleles

Newborn mice and embryos from 7.5 dpc onwards were genotyped by polymerase chain reaction (PCR) or Southern blot of DNA samples prepared from tails, yolk sacs or whole embryos (Fig. 1D; Hogan et al., 1994). In some experiments, embryos at 6.5 and 7.5 dpc were genotyped by PCR after in situ hybridisation. Briefly, embryos were fixed, photographed and incubated in 40 μl of 10 mM Tris-HCl (pH 8.0), 50 mM KCl, 0.5% Tween 20, 0.5% NP-40 and 60 μg of proteinase K for 16-20 hours at 55°C. The proteinase K was heat inactivated at 95°C for 10 minutes and 2 μl of the DNA used for the PCR reaction. Samples were amplified for 40 cycles (94°C for 30 seconds, 58°C for 30 seconds and 72°C for 45 seconds). PCR primers were: H1 (5′-aggccgagtgtgaaatcagag-3′) and H2 (5′-cagaagagctgtggttaaccaa-3′) for the *Hex* wild-type allele; N1 (5′-ctgt-gctcgacgttgtcactgaag-3′) and N2 (5′-tattcggcaagcaggcatcgccat-3′) for the *Neo* gene.

Histology, in situ hybridisation and X-gal staining

For histology, embryos were fixed in Bouins fixative, dehydrated through graded ethanol, embedded in paraffin wax and sectioned. Sections were stained with hematoxylin-eosin as previously described (Kaufman, 1992). In situ hybridisation and X-gal staining of whole-mount embryos used standard procedures (Thomas and Beddington, 1996; Hogan et al., 1994). The following probes were used: *Fgf8* (Crossley and Martin, 1995), *Bf1* (Tao and Lai, 1992), *Nkx2.1* (Lazzaro et al., 1991), *Shh* (Echelard et al., 1993), *Pax6* (Walther and Gruss, 1991), *Hesx1* (Thomas and Beddington, 1996), *Six3* (Oliver et al., 1995), *Cerrl* (Thomas et al., 1997), *Lim1/Lhx1* (Shawlot and Behringer, 1995), *Hnf3β* (Ang et al., 1993), *AFP* (Cascio and Zaret, 1991), *TTF2* (Zannini et al., 1997), *Mrg1/Cited2* (Dunwoodie et al., 1998).

Generation of $Hex^{-/-}$ ES cells and $Hex^{-/-}$<=>$Rosa26^{+/+}$ chimeras

One $Hex^{+/-}$ ES cell clone that transmitted the targeted allele through the germline was used to generate $Hex^{-/-}$ ES cells. $Hex^{+/-}$ ES cells were cultured in medium containing from 2 to 3.5 mg/ml of G418 (Mortensen et al., 1992). Approximately 200 surviving colonies were screened by PCR and Southern blot as described above. Nine clones were found to be homozygous for the *Hex* targeted allele and two of them, which contained 40 chromosomes (Hogan et al., 1994), were used for injections into blastocysts obtained from crossing *Rosa26/Rosa26* males with C57Bl6 females (Fig. 1C; Zambrowicz et al., 1997). Injected blastocysts were transferred into pseudopregnant females and harvested at 9.5 and 10.5 dpc. The degree of chimerism was estimated by X-gal staining (Hogan et al., 1994).

RESULTS

Generation of the *Hex* null mutant mouse

A null mutation in the *Hex* gene was created by homologous recombination in ES cells. Most of exon I and all of exons II and III, containing the homeodomain and a putative repressor domain in the N terminus (Crompton et al., 1992; Tanaka et al., 1999), were replaced by an *IRES-lacZ-Neo* cassette. The *IRES-lacZ* in this construct was under the control of the *Hex* promoter (Fig. 1A).

Heterozygous *Hex* mice were normal and fertile. Intercrosses between heterozygous mice produced no live $Hex^{-/-}$ pups at birth (n=148) but, as summarised in Table 1, genotypic analysis of embryos from 6.5 to 10.5 dpc showed no deviation from the expected Mendelian ratio. However, it appeared that *Hex* homozygotes began to die at about 11.5 dpc, and by 15.5 dpc no $Hex^{-/-}$ embryos were present.

Morphologically, $Hex^{-/-}$ embryos were indistinguishable from heterozygous or wild-type littermates at 6.5 and 7.5 dpc. Embryonic and extraembryonic regions appeared normal and

Table 1. Genotypes of mice resulting from $Hex^{+/-}$ intercrosses

	Genotype			
Stage	+/+	+/−	−/−	Total
7.5 dpc	12	33	14	59
8.5 dpc	28	59	19	106
9.5 dpc	38	78	31	147
10.5 dpc	32	68	28	128
11.5 dpc	9	13	6*	28
12.5 dpc	11	17	7*	35
13.5 dpc	21	12	5*	38
14.5 dpc	6	17	4*	27
15.5 dpc	2	6	0	8
At birth	62	86	0	148

*Some of these represent empty yolk sacs or resorbing embryos.

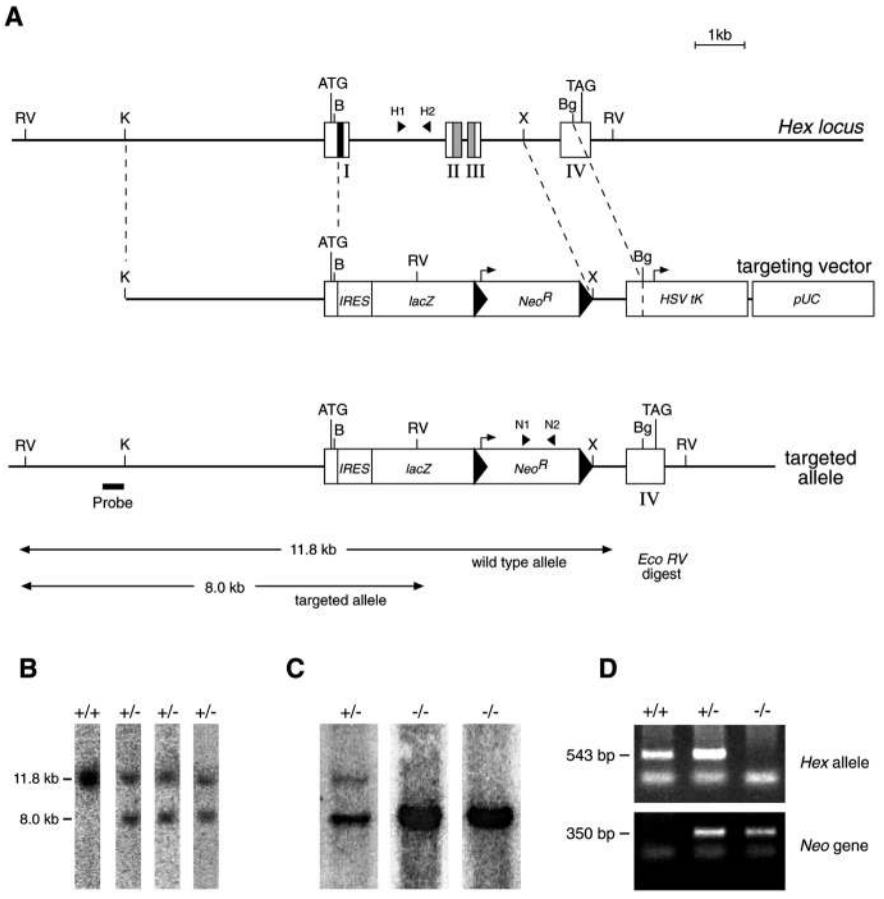

Fig. 1. Generation of the *Hex* null mutant mice. (A) Schematic representations of the mouse wild-type *Hex* locus, targeting vector and targeted allele. The putative repressor domain contained in exon I (solid box) and the homeodomain included in exons II and III (shaded boxes) are shown. The *IRES-lacZ-Neo* cassette and the Herpes simplex virus thymidine kinase gene (*HSV-tk*) in the targeting vector are indicated. Arrows show the direction of transcription. The genomic probe which identifies different *Eco*RV fragment sizes for the wild-type and targeted allele is shown. (B) Southern blot analysis of genomic DNA from wild-type and $Hex^{+/-}$ ES cell clones. (C) Southern blot analysis on genomic DNA from $Hex^{+/-}$ and $Hex^{-/-}$ ES cell clones. (D) PCR genotyping of embryos and adult mice from heterozygous matings. Primers H1-H2 and N1-N2 were used to amplify the *Hex* allele and the *Neo* gene (A).

there was no constriction at the embryonic/extraembryonic boundary. However, at 8.5 dpc $Hex^{-/-}$ embryos showed a reduction in forebrain tissue compared with $Hex^{+/-}$ and wild-type littermates and this reduction became more pronounced later (Fig. 2). Often, $Hex^{-/-}$ mutants were retarded and showed large pericardial cavities.

At 6.5 and 7.5 dpc, no X-gal staining was detected in the AVE or definitive endoderm in $Hex^{-/-}$ embryos. This is due to the deletion of enhancer sequences in the targeted allele (T. R., unpublished observations). β-gal activity was first observed at 8.5 dpc in the vascular system and foregut diverticulum of heterozygous and homozygous mutant embryos. From 9.5 dpc onwards, *lacZ* expression in these two domains, and in the thyroid, could be detected in $Hex^{+/-}$ embryos (Fig. 2G and data not shown). X-gal staining of $Hex^{-/-}$ mutants at 9.5 and 10.5 dpc revealed abnormalities in the thyroid primordium and in the liver (see below).

Variable anterior truncations in the *Hex*$^{-/-}$ embryos

Morphological and histological examination failed to show anterior truncations in headfold and early somite stage $Hex^{-/-}$ mutants. However at the 8-10 somite stage, $Hex^{-/-}$ embryos showed a significant reduction in forebrain tissue. At 9.5 and 10.5 dpc, approximately 90% of $Hex^{-/-}$ embryos displayed some degree of anterior deficiency. According to the extent of these defects, $Hex^{-/-}$ embryos were broadly classified into three groups (Fig. 2A-D). Class I mutant embryos showed a complete lack of telencephalic vesicles, infundibulum, eyes, olfactory placodes and Rathke's pouch (approx. 30% of embryos; Fig. 2B). The first branchial arch was fused in the midline and histological sections revealed that it had no pharyngeal endoderm. Class II mutants showed a less severe phenotype (Fig. 2C). The overall size of the forebrain was significantly reduced but forebrain structures could be identified (approx. 30% of embryos). Telencephalic vesicles were consistently smaller in class II mutants when compared with heterozygous or wild-type littermates. In some class II embryos, optic vesicles were also reduced, but eye defects were less frequent than telencephalic abnormalities. No abnormalities were observed in the first branchial arch of these mutants. Class III mutants had one small telencephalic vesicle and one olfactory placode (approx. 30% of embryos; Fig. 2D). In 10.5 dpc wild-type embryos, the telencephalon is formed by two telencephalic vesicles divided by a dorsal midline. The floor of each telencephalic vesicle is occupied by a developing medial ganglionic eminence. In class III mutants, no dorsal midline or medial ganglionic eminence was observed. In the diencephalon the two eyes were separated by only a short optic stalk. Approximately 10% of $Hex^{-/-}$ mutants did not display evidence of forebrain abnormalities. Anterior defects in the *Hex* mutants appeared to be restricted to the forebrain region and no abnormalities were observed in midbrain, hindbrain or spinal cord.

Anterior truncations are restricted to rostral forebrain in *Hex*$^{-/-}$ embryos

We have used a number of diagnostic genetic markers such as *Fgf8*, *Bf1*, *Nkx2.1*, *Shh* and *Pax6*, to determine the extent of the anterior truncations in $Hex^{-/-}$ mutants. All 3 classes described above were compared to $Hex^{+/-}$ and $Hex^{+/+}$ littermates from 8.5 to 10.5 dpc. In normal embryos at 8.5 dpc, *Fgf8* is expressed in the anterior neural ridge (ANR) and mid-hindbrain boundary (isthmus) (Crossley and Martin, 1995; Shimamura and Rubenstein, 1997). As shown in Fig. 3D, *Fgf8* expression in the ANR was completely abolished in class I

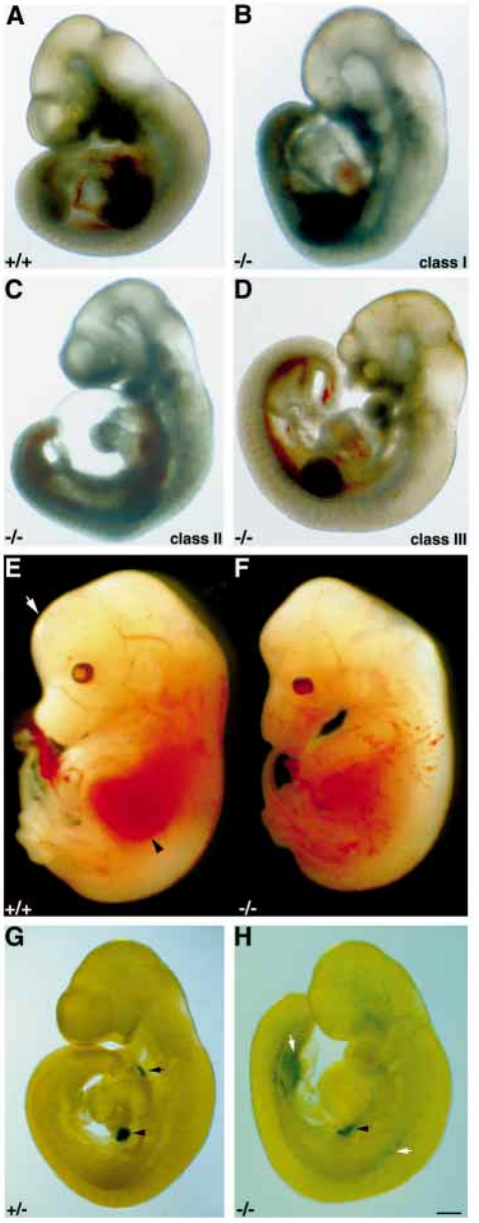

Fig. 2. Phenotype and *lacZ* expression in *Hex*$^{-/-}$ mutants. (A-D) Forebrain defects in the *Hex*$^{-/-}$ mutants at 10.5 dpc. (A) Wild-type embryo. (B) Class I *Hex*$^{-/-}$ embryo showing severe forebrain truncation. (C) Class II *Hex*$^{-/-}$ mutant with small telencephalic vesicles and a large pericardial cavity. (D) Class III *Hex*$^{-/-}$ mutant showing one single telencephalic vesicle and one olfactory placode. Wild-type (E) and *Hex*$^{-/-}$ mutant (F) embryos at 13.5 dpc showing forebrain defects (arrow) and absence of the liver (arrowhead). (G) X-gal staining of *Hex*$^{+/-}$ embryos at 9.5 dpc show β-galactosidase activity in the thyroid primordium (arrow) and liver diverticulum (arrowhead). (H) *Hex*$^{-/-}$ mutant embryos showing X-gal staining in the liver diverticulum (arrowhead) and blood vessels (white arrows). Bar, 250 μm (A-D); 700 μm (E,F); 200 μm (G,H).

mutant embryos (*n*=3). At 9.5 and 10.5 dpc, *Fgf8* is normally expressed in the commissural plate, roof of the diencephalon, infundibulum, olfactory placodes and isthmus. At these stages class I mutants did not express *Fgf8* in the forebrain, but did so normally in the isthmus (*n*=4), indicating that most of the forebrain had been deleted in these mutants (Fig. 3A,B). In class II and III *Hex*$^{-/-}$ mutants, *Fgf8* expression in the forebrain was attenuated in concert with the degree of anterior truncation when compared with normal littermates (*n*=4; Fig. 3E-G). *Bf1* is expressed in the telencephalic vesicles and olfactory placodes of wild-type embryos (Tao and Lai, 1992; Shimamura et al., 1995) but was absent in class I, and markedly reduced in class II and III mutant embryos (Fig. 3H-K). At 10.5 dpc, *Bf1* expression in the telencephalon abuts the dorsal midline and is strongly expressed in the lamina terminalis in wild-type embryos (Furuta et al., 1997; Shimamura et al., 1995). Interestingly, in class III mutants, *Bf1* was expressed throughout the dorsal neural epithelium of the telencephalon and no expression was observed where the lamina terminalis should form (Fig. 3K). Analysis of *Bf1* expression confirmed the presence of only one olfactory placode in these mutants (Fig. 3K). These expression data suggest a failure in the specification of the dorsal midline of the telencephalon in class III mutants.

To investigate the dorsoventral patterning of the forebrain, the expression of *Nkx2.1*, *Shh* and *Pax6* was analysed in *Hex* mutant and normal embryos. *Nkx2.1* is expressed in the ventral diencephalon and the floor of the telencephalon in 9.5 dpc wild-type embryos (Lazzaro et al., 1991; Shimamura et al., 1995). In Class I mutants, *Nkx 2.1* expression was either absent (*n*=3) or markedly reduced (*n*=3; Fig. 4A-D). The posterior limit of *Nkx2.1* forebrain expression at the boundary between the dorsal and ventral thalamus (the zona limitans intrathalamica, ZLI) appeared normal in class II and III mutants (Shimamura and Rubenstein, 1997; Rubenstein et al., 1998). However, the rostral extension of *Nkx2.1* expression domain into the floor of the developing telencephalon was absent in these mutants (*n*=7; Fig. 4E,F). To verify that the ZLI is the posterior limit of the brain phenotype we confirmed in 10.5 dpc wild-type embryos that transcripts of *Shh* accumulate dorsally in the thalamus, thus marking the ZLI (Echelard et al., 1993; Shimamura et al., 1995). This dorsal deflection of *Shh* expression into the ZLI was apparently normal in *Hex*$^{-/-}$ mutants (Fig. 4G,J). However, the *Shh* expression domain in more rostral forebrain was significantly reduced in class I *Hex*$^{-/-}$ embryos (*n*=8; Fig. 4H). Using *Pax6* expression as a marker of the dorsal thalamus and rostral midbrain (Walther and Gruss, 1991), dorsal tissues caudal to the ZLI appeared normal in the *Hex*$^{-/-}$ mutants (Fig. 4K,L). However, rostral to the ZLI the size of the forebrain is markedly reduced in class I mutant embryos when compared with wild-type littermates (*n*=7). The remaining forebrain tissue showed normal dorso-ventral patterning as judged by the distribution of *Pax6* and *Shh* transcripts (Fig. 4G-L). Class II and III embryos showed reduced *Nkx2.1*, *Shh* and *Pax6* expression domains in forebrain territories but dorso-ventral patterning was unaffected (*n*=16; Fig. 4E,F,I,J).

Early patterning of the anterior neural plate in *Hex*$^{-/-}$ mutants

It was important to determine whether the lack of anterior tissue had an early conception, due to a failure of anterior neural induction, or whether the anterior neural plate was induced but not maintained. Two neural markers, *Hesx1* and *Six3* were used as indicators of normal anterior neural plate development, both being expressed in the prospective forebrain

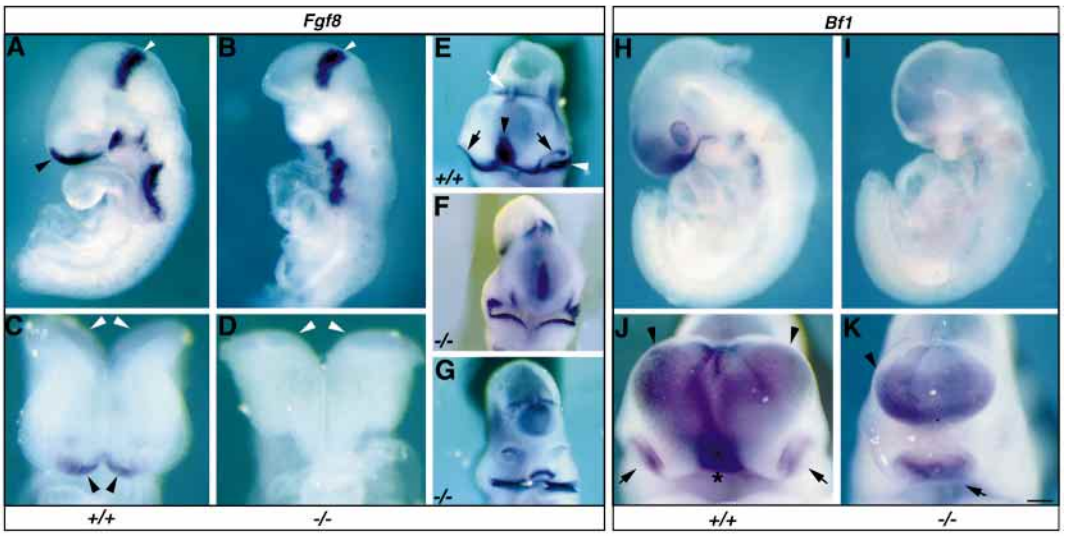

Fig. 3. *Fgf8* and *Bf1* expression in $Hex^{+/+}$ and $Hex^{-/-}$ embryos. (A) Wild-type embryo at 9.0 dpc. *Fgf8* is expressed in the commissural plate (black arrowhead) and isthmus (white arrowhead). (B) Class I $Hex^{-/-}$ mutant at 9.0 dpc devoid of *Fgf8* expression in the commissural plate but with normal expression in the isthmus (white arrowhead). (C) Wild-type embryo at 8.5 dpc showing *Fgf8* expression in the ANR (black arrowheads) and isthmus (white arrowheads). (D) Class I $Hex^{-/-}$ mutant with no *Fgf8* expression in the ANR but normal expression in the isthmus (white arrowheads). (E) Wild-type 10.5 dpc embryo. *Fgf8* expression is observed in the commissural plate (black arrowhead), olfactory placodes (black arrows), roof of the diencephalon (white arrow), and first branchial arch (white arrowhead). (F,G) Class II (F) and III (G) $Hex^{-/-}$ embryos showing reduced or absent *Fgf8* expression in the commissural plate and olfactory placodes. (H) Wild-type 9.5 dpc embryo. *Bf1* is expressed in the telencephalic vesicles, optic and olfactory placodes. (I) Class I 9.5 dpc $Hex^{-/-}$ mutant. No *Bf1* expression is detected in the forebrain region. (J) *Bf1* is expressed in telencephalic vesicles (arrowheads), olfactory placodes (arrows) and the lamina terminalis (asterisk) in a wild-type 10.5 dpc embryo. The dorsomedial region of the telencephalon does not express *Bf1*. (K) Class III $Hex^{-/-}$ embryo. *Bf1* is expressed in a single domain in the telencephalon (arrowhead) and olfactory placode region (arrow), and no *Bf1* expression is observed in the lamina terminalis. Bar, 200 μm (A,B,H,I); 40 μm (C,D); 210 μm (E-G); 120 μm (J,K).

region at 7.5 dpc (Oliver et al., 1995; Hermesz et al., 1996; Thomas and Beddington, 1996). As shown in Fig. 5A,B,E and F, *Hesx1* and *Six3* were expressed normally in the anterior neural plate of $Hex^{-/-}$ embryos from late streak to early somite stages (n=11). However, the *Hesx1* expression domain was significantly reduced in $Hex^{-/-}$ mutants by the 8-10 somite stage (n=4; Fig. 5D). Similarly, *Six3* expression was markedly reduced in $Hex^{-/-}$ embryos by the 3-4 somite stage (n=3; Fig. 5H). Therefore, the prospective forebrain region is correctly induced in $Hex^{-/-}$ embryos as no difference in *Hesx1* and *Six3* expression was observed between $Hex^{-/-}$, $Hex^{+/-}$ or $Hex^{+/+}$ embryos at 7.5 dpc. The later variability in forebrain development must arise at early somite stages, when *Hesx1* and *Six3* expression becomes reduced.

Patterning of the AVE and definitive endoderm in $Hex^{-/-}$ embryos

Hex is expressed in the AVE of pre-streak embryos and, as gastrulation proceeds, expression appears in a second domain of definitive endoderm cells at the tip of the elongating streak (Thomas et al., 1998). Since *Hex* is not expressed in the neural ectoderm, the forebrain defects observed in the $Hex^{-/-}$ mutants might arise from the lack of *Hex* function in the AVE, definitive endoderm or both. The expression of *Cerberus-like* (*Cerrl*) was analysed in *Hex* mutants because *Cerrl* is expressed in the AVE and definitive endoderm in wild-type embryos (Belo et al., 1997; Shawlot et al., 1998; Biben et al., 1998). At pre-streak stages, *Cerrl* expression in the AVE of $Hex^{-/-}$ mutants was indistinguishable from heterozygous or wild-type embryos (n=3). Normally, at mid-streak stages, both *Cerrl* expression domains can be seen (Fig. 6A), but in $Hex^{-/-}$ embryos at this stage only *Cerrl* expression in the AVE is evident (n=2; Fig. 6B). At late streak and early headfold stages, *Cerrl* is expressed in anterior definitive endoderm as well as in prechordal and notochordal plates (Biben et al., 1998). *Cerrl* expression was absent at late streak and early headfold stages in $Hex^{-/-}$ embryos (n=7; Fig. 6D). Normally, *Lim1* is expressed in the AVE and mesodermal wings during streak stages (Shawlot and Behringer, 1995) and this appears unperturbed in $Hex^{-/-}$ mutants (Fig. 6E,F; n=5). *Mrg1/Cited2* is also expressed proximally in the AVE of streak-stage wild-type and $Hex^{-/-}$ embryos (Dunwoodie et al., 1998; data not shown).

Two markers of the axial mesendoderm, *Lim1* and *Hnf3β* (Sasaki and Hogan, 1993; Ruiz i Altaba et al., 1993; Ang et al., 1993; Monaghan et al., 1993; Shawlot and Behringer, 1995) were examined. Late streak $Hex^{-/-}$ embryos showed severely reduced *Lim1* and *Hnf3β* expression in the axial mesendoderm emanating from the node. In contrast, in the node region both *Hnf3β* and *Lim1* expression domains appeared expanded in $Hex^{-/-}$ mutants (n=4; Fig. 6G-L). However, *Hnf3β* expression in the notochord appeared normal when compared with wild-type littermates (Fig. 9A,B). The absence or reduction of *Lim1*, *Hnf3β* and *Cerr1* expression domains in the anterior axial mesendoderm suggest that the patterning and/or morphogenetic movements of this tissue have been compromised in $Hex^{-/-}$ mutants. Together, these data suggest that the AVE was correctly specified in $Hex^{-/-}$ mutants and that the anterior definitive endoderm was the tissue where the primary defect occurred.

Hex is required in definitive endoderm for normal forebrain development

Taking advantage of the developmental bias whereby ES cells injected into a blastocyst tend to colonise only epiblast derivatives (Beddington and Robertson, 1989), chimeras were generated in which the embryo proper was composed

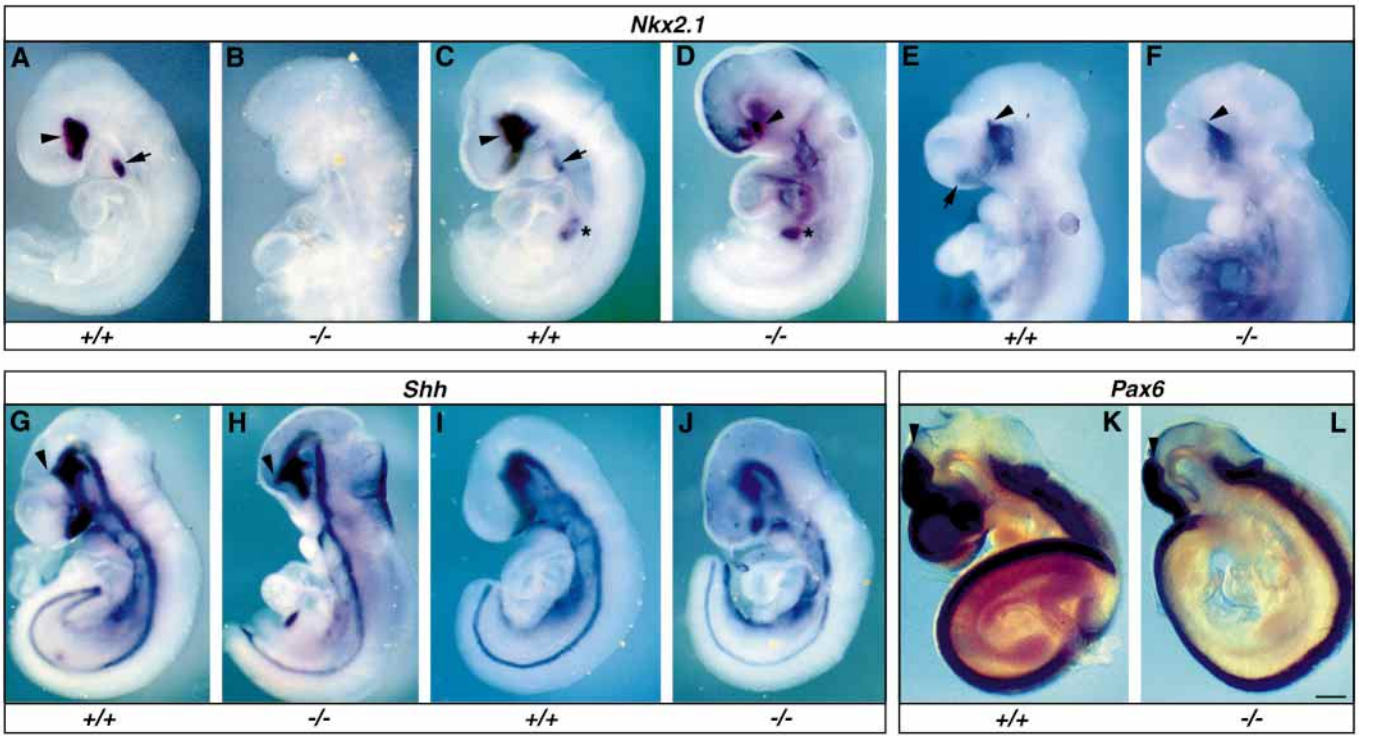

Fig. 4. *Nkx2.1*, *Shh* and *Pax6* expression in $Hex^{+/+}$ and $Hex^{-/-}$ embryos. (A) Wild-type 9.0 dpc embryo. *Nkx2.1* expression is detected in the ventral forebrain (arrowhead) and thyroid primordium (arrow). (B) Class I 9.0 dpc $Hex^{-/-}$ mutant. No *Nkx2.1* expression is observed in the forebrain and thyroid bud. (C) Wild-type 9.5 dpc embryo. *Nkx2.1* is expressed in the diencephalon and floor of the developing telencephalon (arrowhead), the thyroid primordium (arrow) and lung buds (asterisk). (D) Class I 9.5 dpc $Hex^{-/-}$ mutant. *Nkx2.1* expression is restricted to a small domain in the ventral forebrain (arrowhead). *Nkx2.1* is not expressed in the thyroid primordium but it is in the lung buds (asterisk). (E) Wild-type 10.5 dpc embryo. *Nkx2.1* is expressed in the ventral diencephalon and floor of the telencephalon (arrowhead and arrow respectively). (F) Class III $Hex^{-/-}$ embryo. *Nkx2.1* is normally expressed in the diencephalon but is absent in the floor of the telencephalon. Note that the posterior limit of *Nkx2.1* expression appears normal (arrowhead). (G) Wild-type 10.5 dpc embryo. *Shh* expression in the forebrain extends dorsally between the dorsal and ventral thalamus marking the ZLI (arrowhead). (H) Class I 10.5 dpc $Hex^{-/-}$ mutant. *Shh* expression in the ZLI appears normal (arrowhead) but there is no forebrain tissue rostral to the ZLI. (I,J) Wild-type (I) and class II $Hex^{-/-}$ mutant (J) at 10.0 dpc. The *Shh* expression domain rostral to the ZLI appears reduced in the $Hex^{-/-}$ embryo (J) when compared with a wild-type littermate (I). (K) At 10.5 dpc, *Pax6* is normally expressed in dorsal regions of the forebrain and rostral midbrain, with a sharp caudal limit in the latter (arrowhead). (L) Class I 10.5 dpc $Hex^{-/-}$ mutant. *Pax6* expression in the rostral midbrain and caudal forebrain appears normal, but the expression domain in the rostral forebrain is reduced. *Pax6* expression in hindbrain and spinal cord regions is normal in $Hex^{-/-}$ embryos. Bar, 230 μm (A-D); 250 μm (E-L).

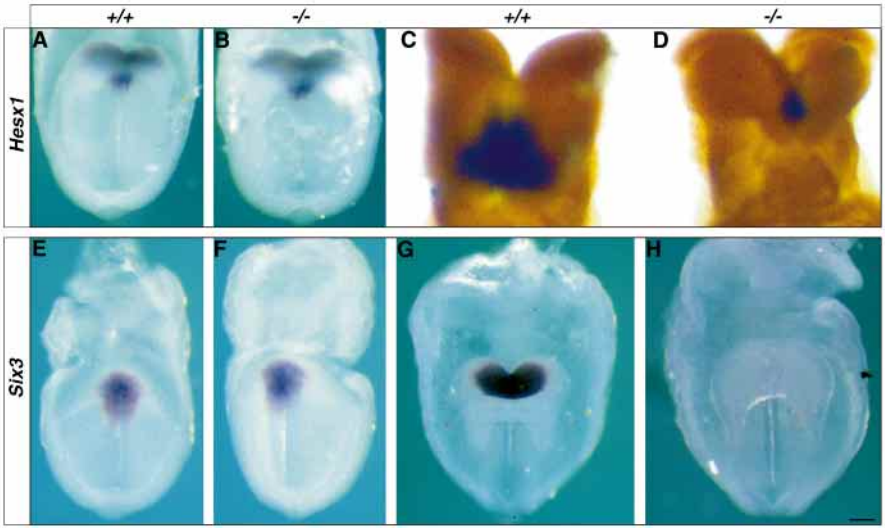

Fig. 5. *Hesx1* and *Six3* expression in $Hex^{+/+}$ and $Hex^{-/-}$ embryos. At late headfold stages, *Hesx1* expression in the prospective forebrain of $Hex^{-/-}$ embryos (B) is undistinguishable from wild-type littermates (A). By the 8-10 somite stage, *Hesx1* expression in the forebrain is markedly reduced in the $Hex^{-/-}$ embryo (D) when compared with a $Hex^{+/+}$ littermate (C). At early headfold stages, *Six3* is expressed in the prospective forebrain in wild-type (E) and $Hex^{-/-}$ (F) embryos. At the 3-5 somite stage, *Six3* expression domain in the $Hex^{-/-}$ mutants (H) is much smaller than that of wild-type littermates (G). Bar, 95 μm (A,B,E-H); 50 μm (C,D).

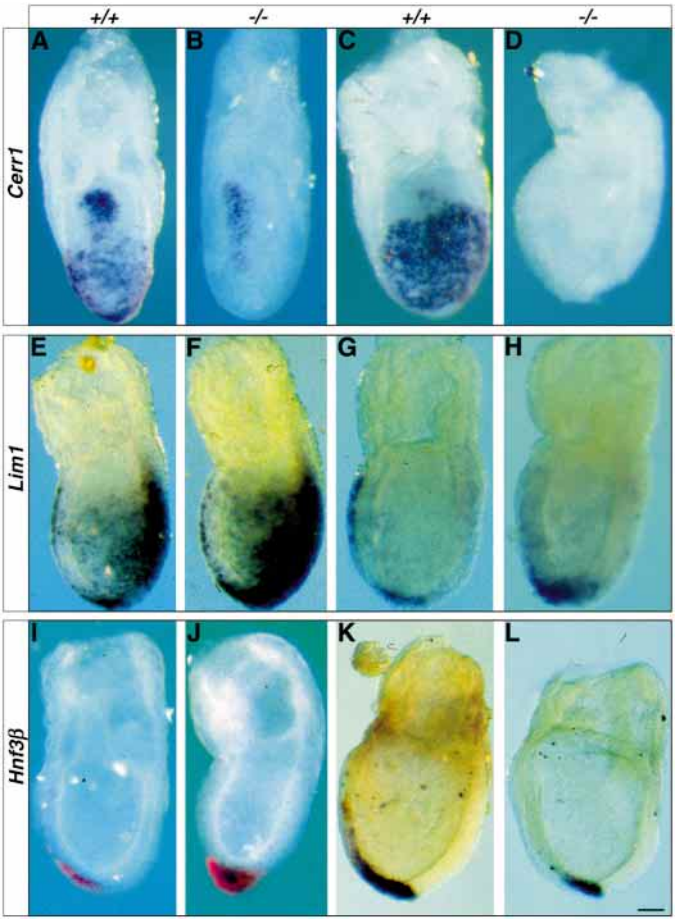

Fig. 6. *Cerrl*, *Lim1* and *Hnf3β* expression in $Hex^{+/+}$ and $Hex^{-/-}$ embryos. At midstreak stages, *Cerrl* is expressed in the AVE and definitive endoderm in the wild-type embryo (A) but is absent in the definitive endoderm of the $Hex^{-/-}$ mutant (B). Late streak wild-type embryo when *Cerrl* is expressed in definitive endoderm, prechordal and notochordal plates (C). There is no *Cerrl* expression in $Hex^{-/-}$ embryos (D). Normal *Lim1* expression in the AVE of wild-type (E) and $Hex^{-/-}$ (F) embryos. At late streak stages, *Lim1* is normally expressed in the axial mesendoderm (G) but is reduced in $Hex^{-/-}$ mutants (H). At late streak and headfold stages, *Hnf3β* is expressed in the node and axial mesendoderm in the wild-type embryo (I,K), but is not in the axial mesendoderm of $Hex^{-/-}$ mutants (J,L). The *Lim1* and *Hnf3β* expression domains in the node appear expanded (H,J). A-C, frontal views; D-L, lateral views (anterior to the left). Bar, 80 μm.

predominantly of $Hex^{-/-}$ tissues and the extraembryonic tissue of wild-type cells. If the primary defect in *Hex* mutants occurs in the definitive endoderm then chimeric concepti, containing predominantly $Hex^{-/-}$ definitive endoderm and wild-type AVE, should display anterior truncations similar to the $Hex^{-/-}$ mutants.

The chimerism rate was assessed by estimating the ratio between blue cells (wild-type *Rosa26*) and white cells ($Hex^{-/-}$ ES cell progeny). Two groups of chimeric embryos were recovered at 9.5 and 10.5 dpc. In one group, embryos were very retarded, had not turned and resembled 8.5 dpc embryos. Despite the small size of the embryo, the size of the yolk sac was similar to that from non-chimeric littermates. These embryos were highly populated by $Hex^{-/-}$ cells as judged by

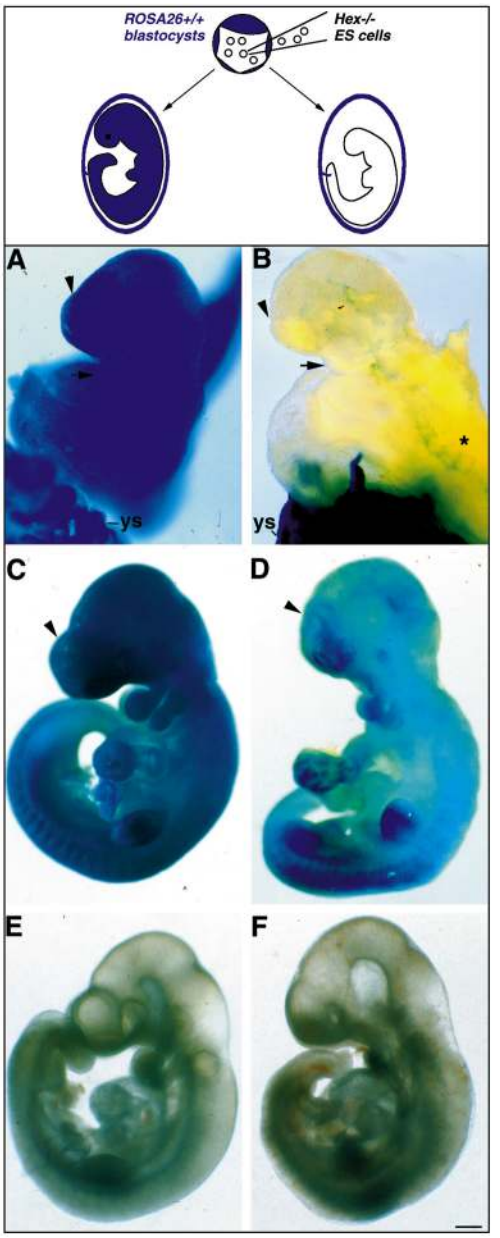

Fig. 7. Anterior defects in $Hex^{-/-}$ ES cells⇔$Rosa26^{+/+}$ chimeric embryos. (A) X-gal stained non-chimeric embryo at 9.0 dpc with a normal forebrain (arrowhead) and first branchial arch (arrow). (B) X-gal-stained chimeric embryo showing abnormal development of the forebrain (arrowhead) and the first branchial arch (arrow). β-galactosidase activity in the embryo marks the aorta and intersomitic vessels (asterisk) where *Hex* is normally expressed. The yolk sac (ys) is blue because the visceral endoderm is composed of *Rosa26* cells. 9.5 dpc non-chimeric (C) and chimeric (D) embryos after X-gal staining. In the chimera the telencephalic vesicles are small. 9.5 dpc non-chimeric (E) and chimeric (F) embryos. Again, the forebrain is reduced in the chimeric embryo. (Chimerism demonstrated by subsequent X-gal staining). Bar, 190 μm.

X-gal staining and showed forebrain abnormalities (n=10; Fig. 7B). However, since normal development was impaired in these chimeras, it was difficult to determine whether anterior defects were due to the presence of $Hex^{-/-}$ mutant cells in the definitive endoderm or whether they resulted from

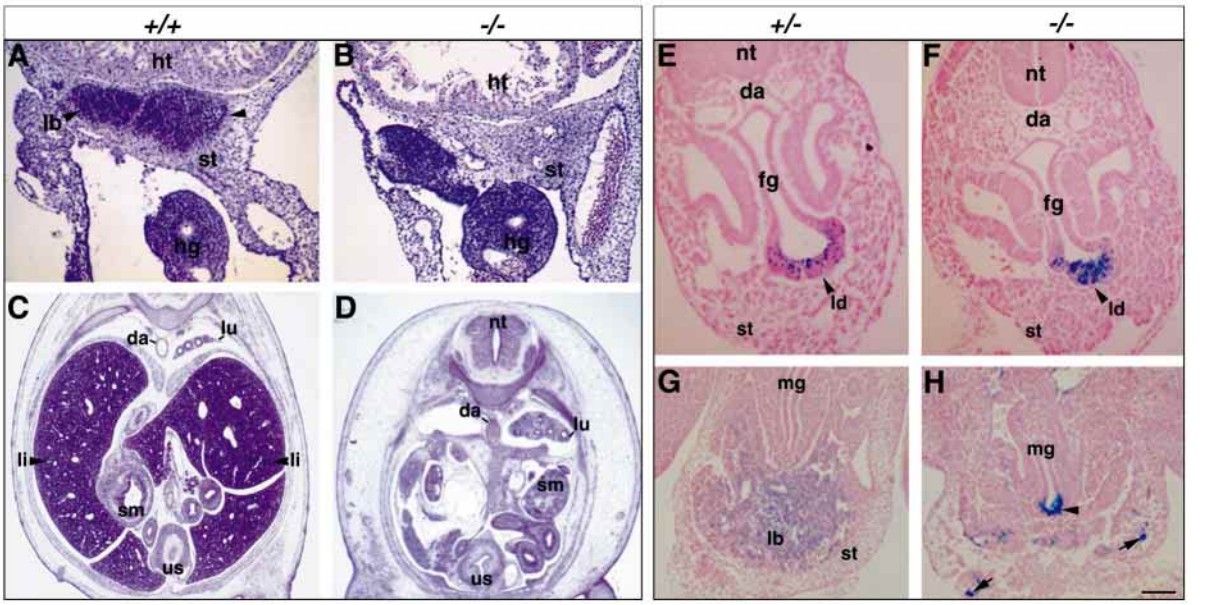

Fig. 8. Defective liver formation in the *Hex*$^{-/-}$ embryos. (A-D) Transverse sections of wild-type and *Hex*$^{-/-}$ embryos stained with hematoxylin-eosin. At 10.5 dpc, the developing liver bud is recognizable within the septum transversum in the wild-type embryo (A; arrowheads) but is absent in the *Hex*$^{-/-}$ mutant (B). At 13.5 dpc, the liver is a prominent organ in the abdominal cavity of the wild-type embryo (C; arrowheads) but is not observed in the *Hex*$^{-/-}$ mutant (D). Transverse sections of X-gal stained *Hex*$^{+/-}$ (E) and *Hex*$^{-/-}$ (F) embryos showing β-galactosidase activity in the liver diverticulum (arrowhead). At 10.5 dpc, the liver bud has expanded and colonised the septum tranversum in the *Hex*$^{+/-}$ embryo (G) but has degenerated in the *Hex*$^{-/-}$ mutant (H; arrowhead). Stained blood vessel endothelial cells are evident in *Hex*$^{-/-}$ embryos (H; arrows). da, dorsal aorta; fg, foregut; hg, hindgut; ht, heart; lb, liver bud; ld, liver diverticulum; li, liver; lu, lung; mg, midgut; sm, stomach; st, septum transversum; us, urogenital sinus. Bar, 125 μm (A,B); 820 μm (C,D); 85 μm (E-H).

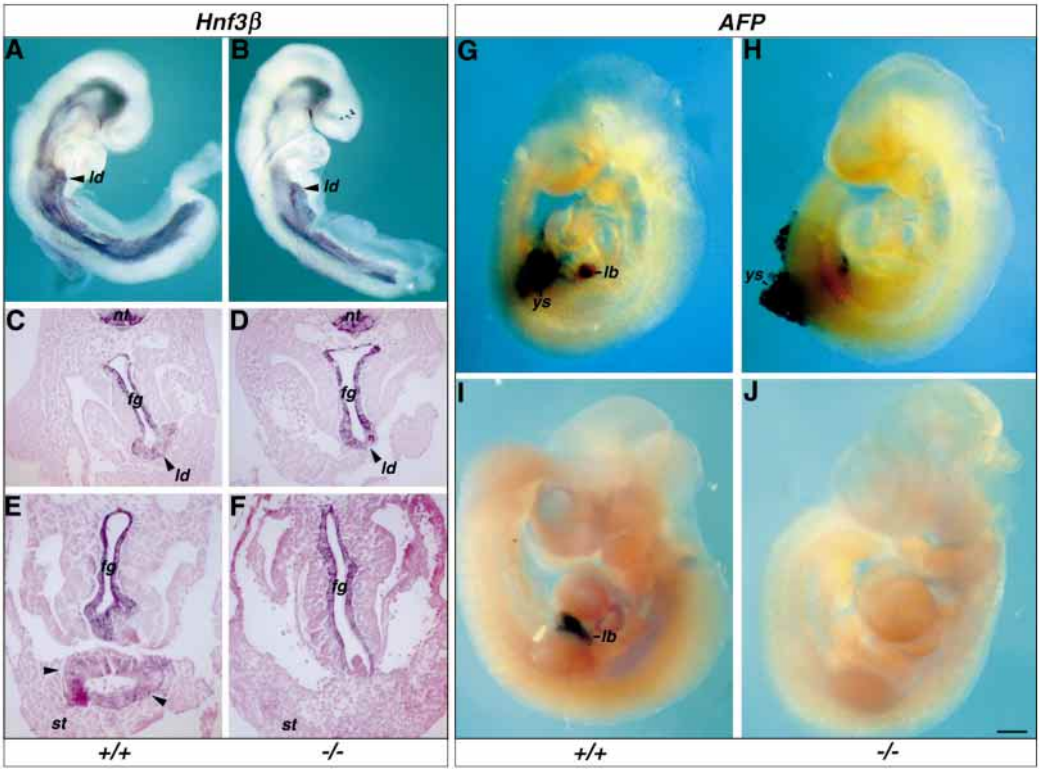

Fig. 9. *Hnf3β* and *AFP* expression in *Hex*$^{+/+}$ and *Hex*$^{-/-}$ embryos. At 9.0 dpc, *Hnf3β* expression in the liver diverticulum (arrowhead) of the *Hex*$^{-/-}$ mutant (B) is normal when compared with the wild-type littermate (A). Transverse sections of a 9.5 dpc wild-type embryo (C) and a *Hex*$^{-/-}$ mutant (D) showing *Hnf3β* expression in the ventral neural tube, foregut and liver diverticulum. At 10.5 dpc, the liver diverticulum has grown into the septum transversum of the wild-type embryo and continues to express *Hnf3β* (E). In the *Hex*$^{-/-}$ mutant at 10.5 dpc, *Hnf3β* is expressed in the foregut but not within the septum transversum (F). At 9.5 (G) and 10.5 dpc (I), *AFP* is expressed in the yolk sac and liver bud of the wild-type embryos but not in the liver bud of the *Hex*$^{-/-}$ mutants (H,J). fg, foregut; ld, liver diverticulum; lb, liver bud; nt, neural tube; st, septum transversum; ys, yolk sac. Bar, 250 μm (A,B,G-J); 130 μm (C,D); 100 μm (E,F).

developmental arrest at 8.5 dpc. The reason for this developmental arrest is unknown, since 2 independent $Hex^{-/-}$ ES cell clones gave rise to the same type of chimeras. The second group of chimeras, where the contribution of wild-type cells was higher (n=8; Fig. 7D), were more informative. These chimeric embryos were comparable to non-chimeric littermates but they displayed anterior defects in the forebrain that were very similar, if not identical, to those shown in class II $Hex^{-/-}$ mutant embryos (Figs 7D,F, 2C). Therefore, *Hex* function in the definitive endoderm is required for normal forebrain development.

Liver defects in *Hex*$^{-/-}$ embryos

In mouse, hepatic differentiation begins at about the 6 somite stage (8.5 dpc) when signals from the cardiac mesoderm induce a discrete region of the foregut to express specific hepatocyte proteins, such as albumin and α-fetoprotein (AFP) (Zaret, 1998). Cells in this foregut diverticulum then begin to proliferate and by 9.5 dpc they migrate, in a cord-like fashion, into the mesenchyme of the septum transversum, forming the liver bud. At 10.5 dpc, the liver bud becomes a vascularised organ and hematopoietic precursor cells take up residence there.

Hex expression is detected in the foregut diverticulum at the time when liver specification occurs and it continues to be expressed in the liver throughout fetal and adult life (Thomas et al., 1998; Tanaka et al., 1999). To check the integrity of the liver bud we examined serial histological sections of $Hex^{-/-}$, $Hex^{+/-}$ and wild-type embryos from 10.5 to 13.5 dpc. At 13.5 dpc, a normal liver was observed in $Hex^{+/+}$ and $Hex^{+/-}$ embryos but this organ was absent in $Hex^{-/-}$ mutants (Figs 2E,F, 8C,D). At 10.5 dpc, the liver bud could be recognised in the septum transversum of wild-type embryos (Fig. 8A). However, no sign of liver parenchyma was ever seen in the septum of $Hex^{-/-}$ embryos (n=18; Fig. 8B). At 8.5 and 9.5 dpc, the liver diverticulum could be identified in both $Hex^{+/-}$ and $Hex^{-/-}$ embryos as a small region of X-gal positive cells in the ventral foregut (Figs 2G,H, 8E,F). By 10.5 dpc, the liver bud had expanded significantly in the $Hex^{+/-}$ embryos and many X-gal positive cells had invaded the septum transversum (Fig. 8G). In contrast, in $Hex^{-/-}$ mutants the liver diverticulum appeared thin and no sign of migration of hepatocytes into the septum was observed (Fig. 8H). These data suggest that the initial step of specification of the foregut diverticulum takes place and proliferation of liver precursors is initiated. However, the migration of these cells into the septum fails and the liver diverticulum subsequently degenerates.

We examined the expression of some diagnostic markers of liver differentiation in $Hex^{-/-}$, $Hex^{+/-}$ and $Hex^{+/+}$ embryos. *Hnf3β* is expressed in the foregut diverticulum at the time this tissue is specified by cardiac signals and it has been used as a marker for this inductive process (Nishina et al., 1999). *Hnf3β* was expressed normally in the foregut diverticulum of $Hex^{-/-}$ mutant embryos at 8.5 dpc (Fig. 9A,B). Histological sections of whole-mount *Hnf3β* in situ hybridisations at 9.5 dpc, showed comparable levels of *Hnf3β* expression in the foregut diverticulum in all littermates (Fig. 9C,D). However by 10.5 dpc, unlike wild-type embryos, in $Hex^{-/-}$ mutants *Hnf3β* expression in the septum was absent (Fig. 9E,F). In wild-type embryos, *AFP* transcripts were first detected by in situ hybridisation in the foregut diverticulum at 9.5 dpc (Fig. 9G). In contrast, no *AFP* expression was observed in the liver region of $Hex^{-/-}$ mutants at 9.5 or 10.5 dpc (Fig. 9H,J). These data suggest that initial liver specification occurs in $Hex^{-/-}$ mutants but liver organogenesis fails later.

Thyroid defects in *Hex*$^{-/-}$ mutants

In mouse, morphogenesis of the thyroid gland begins at 8.5-9.5 dpc when a small region of the floor of the pharyngeal endoderm invaginates to form the thyroid bud. Some genes, such as *Hex* (Thomas et al., 1998), *Nkx2.1* (Lazzaro et al., 1991) and *TTF2* (Zannini et al., 1997), are expressed in the thyroid bud soon after its formation. Later, the thyroid bud migrates dorso-caudally to its final position anterior to the trachea where it merges with other cell types and begins to differentiate (Macchia et al., 1999). No morphological defects were observed in the thyroid of $Hex^{+/-}$ mutants. The thyroid primordium was either absent in class I $Hex^{-/-}$ mutants, or hypoplastic in class II and III mutants (n=18; Fig. 10A,B). *Nkx2.1* is expressed in the thyroid primordium at 9.5 dpc and

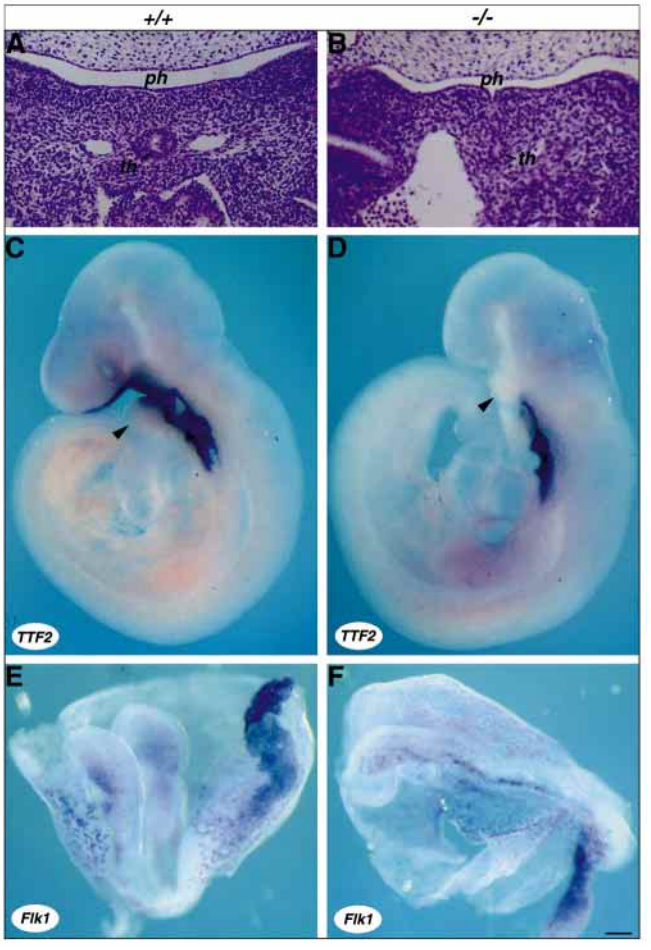

Fig. 10. Development of the thyroid and vascular system in $Hex^{-/-}$ mutants. The thyroid primordium is evident in a wild-type embryo (A) ventral to the pharynx. It is hypoplastic and remains connected to the floor of the pharyngeal endoderm in a $Hex^{-/-}$ embryo (B). *TTF2* expression in wild-type (C) and $Hex^{-/-}$ (D) embryos. *TTF2* is not expressed rostral to the first branchial arch in mutants (arrowhead). *Flk1* expression appears normal in blood vessels of the embryo and yolk sac in wild-type (E) and $Hex^{-/-}$ (F) embryos. Bar, 50 μm (A,B); 160 μm (C,D); 130 μm (E,F).

plays a critical role in thyroid formation (Kimura et al., 1996, 1999). *Nkx2.1* expression, judged in whole-mount and histologically, was absent in the thyroid bud but appeared normal in the lung buds of $Hex^{-/-}$ mutants (n=11; Fig. 4A-D). *TTF2*, which is necessary for early thyroid morphogenesis (De Felice et al., 1998), is expressed in the thyroid primordium, most of the anterior foregut endoderm and oral ectoderm in wild-type 9.5 dpc embryos (Fig. 10C). In $Hex^{-/-}$ mutants, no *TTF2* expression was observed in the thyroid bud (n=5; Fig. 10D). These data suggest that *Hex* function is required at an early stage of thyroid development.

Cardiovascular system in $Hex^{-/-}$ embryos

Hex is transiently expressed in the nascent blood islands of the visceral yolk sac and later in the embryonic angioblasts and endocardium (Thomas et al., 1998). Histologically, apart from the large pericardial cavities, the cardiovascular system of $Hex^{-/-}$ embryos from 8.5 to 14.5 dpc appeared normal (data not shown). *Flk1* encodes a receptor tyrosine kinase that is expressed during endothelial cell differentiation (Yamaguchi et al., 1993; Shalaby et al., 1997) and its expression was not perturbed in $Hex^{-/-}$ mutants (Fig. 10E,F). Tests on the normality of hemopoietic precursors were not undertaken.

In *Xenopus* overexpression of *XHex* leads to the disruption of vascular structures and an increase in the number of vascular endothelial cells, suggesting a role in cellular proliferation of pre-endothelial cells (Newman et al., 1997). It is possible that other factors could compensate for the lack of this *Hex* function in the $Hex^{-/-}$ embryos.

DISCUSSION

Hex function in the liver and thyroid

The results demonstrate that *Hex* is required at an early stage of liver and thyroid gland development. Histological and in situ hybridisation (*Hnf3β*) analysis of $Hex^{-/-}$ mutants showed that the liver diverticulum is formed normally at 8.5 and 9.5 dpc. However, by 10.5 dpc it appeared thin and there was no cell migration into the septum transversum (Figs 8 and 9). This arrest of cell migration was associated with the absence of *AFP* expression in the liver region, indicating that hepatocyte differentiation is disrupted in $Hex^{-/-}$ mutants. The liver defects were 100% penetrant in the $Hex^{-/-}$ embryos. These findings concur with experiments in rats, which suggest that *Hex* may be involved in hepatocyte differentiation rather than growth (Tanaka et al., 1999). Gene targeting studies in mice have identified a number of genes required in early steps of liver differentiation (see Zaret, 1998; Nishina et al., 1999). Some transcription factors such as *Hnf3β* and *GATA4* are required for morphogenesis of the foregut endoderm. In *Hnf3β* and *GATA4* mutant embryos the foregut diverticulum is not formed. Other genes, such as *c-jun*, *Hlx*, *scatter factor/hepatocyte growth factor (SF/HGF)*, *c-met* and *SEK1/MKK4* are involved in expansion and further differentiation of the liver bud. In embryos homozygous for mutations in these genes, the foregut diverticulum is correctly specified and a liver bud is formed, but subsequently (approx. 12.5 dpc) the fetal liver is small and there is hepatocyte apoptosis. *Hex* appears to be the first example of a gene required for the early differentiation of hepatocytes.

The thyroid primordium in $Hex^{-/-}$ mutants at 10.5 dpc was either aplastic or hypoplastic, and no thyroid gland was observed at 13.5 dpc (Fig. 10A,B). The expression of the earliest thyroid marker, *Nkx2.1*, which is essential for thyroid morphogenesis (Kimura et al., 1996, 1999; Macchia et al., 1999), was abolished in $Hex^{-/-}$ mutants at 9.5 and 10.5 dpc (Fig. 4A-D). Likewise, *TTF2* (De Felice et al., 1998) expression was also absent in the $Hex^{-/-}$ mutants (Fig. 10D). However, β-gal activity was detected in the thyroid primordium of $Hex^{-/-}$ mutants at 9.5 dpc, indicating that the primordium was induced in these embryos (data not shown). These data suggest that *Hex* is required at a very early step of thyroid formation.

Forebrain defects in $Hex^{-/-}$ mutants

Several neural markers, at 7.5-10.5 dpc, were used to characterise the extent and timing of the brain defects suffered by $Hex^{-/-}$ mutants. During neural plate and headfold stages, *Hesx1* and *Six3* expression in the prospective forebrain of $Hex^{-/-}$ mutants is indistinguishable from $Hex^{+/-}$ and wild-type littermates (Fig. 5A,B,E,F). It is not until the 3-5 somite stage that $Hex^{-/-}$ mutants can be identified by a reduction of *Hesx1* and *Six3* expression in the anterior neural tissue (Fig. 5C,D,G,H). These data indicate that the presumptive forebrain region is correctly patterned at 7.5 dpc but is reduced 12 hours later in $Hex^{-/-}$ mutants. Other homeobox genes such as *Hnf3β*, *Lim1* and *Otx2* have been shown to be essential for murine brain formation (see Beddington and Robertson, 1999). Embryos homozygous for mutations in any of these genes have deletions of the forebrain, midbrain and rostral hindbrain. These deletions originate early during development and are evident at 7.5 dpc by the absence or reduction of forebrain and midbrain markers such as *Six3*, *Pax2* (Acampora et al., 1998; Rhinn et al., 1998), *Otx2* and *En* (Ang and Rossant, 1994; Shawlot and Behringer, 1995). Thus, the brain defects observed in $Hex^{-/-}$ embryos are clearly different from those in *Hnf3β*, *Lim1* and *Otx2* mutants, both in the extent of the truncation and regarding the stage at which they occur. Only at 8.5 dpc are the forebrain defects in $Hex^{-/-}$ mutants detectable, and 2 days later the spectrum of forebrain truncations can range from none to a severe lack of forebrain tissue (Fig. 2A-D).

Even in the most severely affected $Hex^{-/-}$ mutants no brain defects were observed caudal to the ZLI, the boundary between the dorsal and ventral thalamus (Fig. 4E-L). In vitro experiments indicate that the ZLI subdivides the forebrain into two regions which respond differently to FGF8 signalling (Rubenstein et al., 1998; Martinez et al., 1999). Anterior to the ZLI, FGF8 induces expression of *Bf1*, a gene essential for normal growth and differentiation of the telencephalon (Xuan et al., 1995; Shimamura and Rubenstein, 1997). Caudal to the ZLI, FGF8 induces the *Engrailed* genes and *Pax5* and the hindbrain marker *Gbx2* (Shimamura and Rubenstein, 1997; A. Liu et al., 1999). FGF8 can induce ectopic midbrain and rostral hindbrain when misexpressed in the caudal forebrain (Crossley et al., 1996; A. Liu et al., 1999). At early somite stages, *Fgf8* is expressed in the anterior neural ridge (ANR), the junction between the most anterior neural plate and the non-neural ectoderm. Ablation of the ANR, and tissue recombination experiments in mouse and rat suggest that this signalling centre is required for the induction and/or maintenance of *Bf1*

expression in the anterolateral neural plate, and for the specification of dopaminergic neurons in the rostral forebrain. FGF8 can substitute for the ANR in both these respects (Shimamura and Rubenstein, 1997; Ye et al., 1998). In *Hex*$^{-/-}$ mutants, *Fgf8* expression in the ANR is absent or significantly reduced by the 8-10 somite stage (Fig. 3A-D). The extent and timing of the forebrain defects in *Hex* mutants appear to fit with a disturbance of the *Fgf8* expression in the ANR, and the variability of the rostral defects in *Hex*$^{-/-}$ mutants may reflect the amount of FGF8 signalling that persists. Certainly, embryos carrying an *Fgf8* hypomorphic allele display variable forebrain defects, including small telencephalic vesicles and absence, or reduction, of the dorsal midline septum of the telencephalon (Meyers et al., 1998). Likewise, *Hesx1* and *Oto* mutants show forebrain defects associated with a reduction of *Ffg8* expression in the ANR (Dattani et al., 1998; Zoltewicz et al., 1999). The forebrain defects observed in these mutants are very similar to those observed in class II and III *Hex*$^{-/-}$ embryos. One prediction would be that total absence of *Fgf8* expression in the ANR results in deletion of the forebrain tissue anterior to the ZLI as in class I *Hex*$^{-/-}$ mutants.

Hex function in the AVE and definitive endoderm

The anterior defects in the forebrain of *Hex*$^{-/-}$ mutants cannot be due to a requirement for *Hex* function in the anterior neural tissue since *Hex* is not expressed in the neurectoderm (Thomas et al., 1998). The expression of *Cerrl*, *Lim1* and *Mrg1/cited2* in the AVE was unaffected in *Hex*$^{-/-}$ embryos (Fig. 6). However *Cerrl* expression in the definitive endoderm was completely abolished in the *Hex*$^{-/-}$ mutants indicating that it is the definitive endoderm in which the primary defect occurs. *Hex* and *Cerrl* seem to be coexpressed in the endoderm in the presumptive node region at midstreak stages. However, as gastrulation proceeds, *Hex* is restricted to the midline anterior definitive endoderm (ADE), whilst *Cerrl* is expressed in midline and lateral ADE, as well as in prechordal and notochordal plates (Belo et al., 1997; Shawlot et al., 1998; Biben et al., 1998; Thomas et al., 1998). Thus, lack of *Hex* function in the ADE appears to affect the expression of *Cerrl* in domains where *Hex* is not expressed. This suggests that *Hex* may regulate *Cerrl* expression in a population of precursor cells in the presumptive node region. The existence of common precursors for ADE, prechordal and notochordal plates has been proposed before (Beddington, 1994; Tam and Behringer, 1997) and is supported by fate maps at mid-streak stages (Lawson et al., 1991). Alternatively, *Hex*-expressing cells in the ADE could be required non-cell-autonomously for activation of *Cerrl* expression in the axial mesendoderm. Whichever is the case, it is clear that the specification of axial mesendoderm (ADE, prechordal and notochordal plates) is impaired in *Hex*$^{-/-}$ mutants. Anterior axial mesendoderm also appears abnormal with respect to its reduced or absent *Lim1* and *Hnf3β* expression in late streak and early headfold *Hex*$^{-/-}$ embryos (Fig. 6G-L). At the same time, the expression domains of these markers in the node region was expanded. *Hnf3β* expression was normal in the notochord by the early somite stage in *Hex*$^{-/-}$ mutants, indicating that more posterior axial mesendoderm was properly specified. This may explain why the anterior truncations in the *Hex* mutants are restricted to the rostral forebrain whilst in the *Hnf3β* and *Lim1* mutants the entire forebrain, midbrain and rostral hindbrain are absent. It is possible that only the anterior most cell populations of the axial mesendoderm are affected in the *Hex*$^{-/-}$ mutants, which might correspond with the ADE and the prechordal plate region. In favour of this interpretation is the observation that the anterior truncations in the *Hex* mutants have a posterior boundary at the ZLI, which has been suggested to coincide with the end of the notochord and the beginning of the prechordal plate (Shimamura et al., 1995; Shimamura and Rubenstein, 1997; Rubenstein et al., 1998). Hence, alongside the specification defects, the normal morphogenetic movements of anterior axial mesendoderm may be disturbed in *Hex*$^{-/-}$ mutants.

The normal specification of the AVE in *Hex*$^{-/-}$ mutants contrasts with the situation in *Hnf3β*, *Lim1* and *Otx2* mutant embryos. In *Lim1*$^{-/-}$ embryos at 7.5 dpc, the *Cerrl* expression domain is reduced and located near the distal tip of the embryo, presumably in cells that may correspond to the AVE (Shawlot et al., 1998). In *Otx2*$^{-/-}$ mutants not only *Cerrl* but also *Lim1* and *Hesx1* expression domains in the AVE are abnormally localized at the distal region of the embryo at 6.5 dpc (Acampora et al., 1998; Rhinn et al., 1998). Although expression of AVE markers in *Hnf3β* mutants has not been reported, 6.5 dpc *Hnf3β*$^{-/-}$ embryos show accumulation of visceral endodermal cells at the distal tip of the embryo (Ang and Rossant, 1994), which may be due to a disturbance in normal cell movements that move distal visceral endoderm at 5.5 dpc to an anterior-proximal position at the onset of gastrulation (Beddington and Robertson, 1999). This mislocalization of the AVE results in a failure to induce anterior neural plate, indicated by the lack of forebrain and midbrain markers in the *Hnf3β*, *Lim1* and *Otx2* mutants at 7.5 dpc (Shawlot and Behringer, 1995; Acampora et al., 1998; Rhinn et al., 1998), and this seems to go hand in hand with an abnormal constriction at the embryonic/extraembryonic boundary. Wild-type visceral endoderm can rescue this constriction and reverse the early anterior neural defects in chimeric embryos at 7.5 dpc (Dufort et al., 1998; Rhinn et al., 1998). In the *Hex*$^{-/-}$ mutants, the AVE markers *Cerrl*, *Lim1* and *Mrg1* are normally expressed, no constriction at the embryonic/extraembryonic boundary occurs and the anterior neural ectoderm is correctly induced and specified. Therefore, *Hex* is most likely not required in the AVE for normal forebrain formation.

However, *Hex*$^{-/-}$ mutant embryos showed no *Cerrl* expression in ADE. Moreover, injection of *Hex*$^{-/-}$ ES cells into wild-type blastocysts produced chimeric embryos with forebrain defects similar to those observed in the *Hex*$^{-/-}$ mutants. Since it has been shown that injected ES cells give rise predominantly to epiblast-derived tissues but very rarely colonise the visceral endoderm, these chimeric studies indicate that *Hex* is required in the definitive endoderm for normal forebrain development. The reduction in *Fgf8* expression in the ANR may account for the forebrain defects seen in *Hex*$^{-/-}$ mutants, but how this anterior signalling centre is disrupted in the *Hex*$^{-/-}$ mutants is not known. One possibility is that the disturbance in the specification and migration of the anterior axial mesendoderm in *Hex*$^{-/-}$ embryos is responsible for the defects in the ANR. Tissue recombination experiments in mouse have shown that anterior axial mesendoderm is essential for induction and maintenance of *Otx2* expression in the anterior neural ectoderm (Ang et al., 1994). Recently, evidence has been provided of an important role for *Lim1* and *Oto* in the

axial mesendoderm for maintenance of anterior character of the neural ectoderm and head formation (Shawlot et al., 1999; Zoltewicz et al., 1999). The analysis of the *Hex*$^{-/-}$ mutants suggests that the ADE could be exerting a more direct effect on the overlying neurectoderm than believed hitherto. The sequence of inductive steps required to make forebrain may be that the AVE, in synergy with the early node organizer, initiates the induction and patterning of the forebrain, the axial mesendoderm emanating from the node maintains and refines this initial pattern (Ang et al., 1994; Thomas and Beddington, 1996; Acampora et al., 1998; Tam and Steiner, 1999; Shawlot et al., 1999; P. Liu et al., 1999). Subsequently, local signalling centres (like the ANR) are established in the forebrain region to complete the differentiation of the forebrain anlage (Rubenstein et al., 1998). The results presented in this study provide evidence for an essential role of *Hex* in the ADE for the maintenance of anterior identity and formation of an *Fgf8* signalling centre in the rostral neural plate.

We are grateful to K. Zaret and A. Gould for helpful discussions and S. Hodges, P. Dawson, K. Mathers and E. Gregorieva for invaluable technical assistance. We also thank S. Dunwoodie and A. Stewart for help with the ES cells; A. Brown and L. Wiedemann for sequencing the *Hex* genomic clone; and G. Martin, A. MacMahon, R. Di Lauro, P. Gruss, S.-L. Ang, A. Simeone, J. Rossant, R. Behringer and K. Zaret for probes.

REFERENCES

Acampora, D., Avantaggiato, V., Tuorto, F., Briata, P., Corte, G. and Simeone, A. (1998). Visceral endoderm-restricted translation of *Otx1* mediates recovery of *Otx2* requirements for specification of anterior neural plate and normal gastrulation. *Development* **125,** 5091-5104.

Ang, S. L., Wierda, A., Wong, D., Stevens, K. A., Cascio, S., Rossant, J. and Zaret, K. S. (1993). The formation and maintenance of the definitive endoderm lineage in the mouse: involvement of HNF3/forkhead proteins. *Development* **119,** 1301-1315.

Ang, S. L., Conlon, R. A., Jin, O. and Rossant, J. (1994). Positive and negative signals from mesoderm regulate the expression of mouse *Otx2* in ectoderm explants. *Development* **120,** 2979-2989.

Ang, S. L. and Rossant, J. (1994). HNF-3β is essential for node and notochord formation in mouse development. *Cell* **78,** 561-574.

Beddington, R. S. (1994). Induction of a second neural axis by the mouse node. *Development* **120,** 613-620.

Beddington, R. S. and Robertson, E. J. (1989). An assessment of the developmental potential of embryonic stem cells in the midgestation mouse embryo. *Development* **105,** 733-737.

Beddington, R. S. and Robertson, E. J. (1999). Axis development and early asymmetry in mammals. *Cell* **96,** 195-209.

Bedford, F. K., Ashworth, A., Enver, T. and Wiedemann, L. M. (1993). HEX: a novel homeobox gene expressed during haematopoiesis and conserved between mouse and human. *Nucl. Acids Res.* **21,** 1245-1249.

Belo, J. A., Bouwmeester, T., Leyns, L., Kertesz, N., Gallo, M., Follettie, M. and De Robertis, E. M. (1997). Cerberus-like is a secreted factor with neutralizing activity expressed in the anterior primitive endoderm of the mouse gastrula. *Mech. Dev.* **68,** 45-57.

Biben, C., Stanley, E., Fabri, L., Kotecha, S., Rhinn, M., Drinkwater, C., Lah, M., Wang, C., Nash, A., Hilton, D., Ang, S. L., Mohun, T. and Harvey, R. P. (1998). Murine cerberus homologue *mCer-1*: a candidate anterior patterning molecule. *Dev. Biol.* **194,** 135-151.

Cascio, S. and Zaret, K. S. (1991). Hepatocyte differentiation initiates during endodermal-mesenchymal interactions prior to liver formation. *Development* **113,** 217-225.

Crompton, M. R., Bartlett, T. J., MacGregor, A. D., Manfioletti, G., Buratti, E., Giancotti, V. and Goodwin, G. H. (1992). Identification of a novel vertebrate homeobox gene expressed in haematopoietic cells. *Nucl. Acids Res.* **20,** 5661-7.

Crossley, P. H. and Martin, G. R. (1995). The mouse *Fgf8* gene encodes a family of polypeptides and is expressed in regions that direct outgrowth and patterning in the developing embryo. *Development* **121,** 439-451.

Crossley, P. H., Martinez, S. and Martin, G. R. (1996). Midbrain development induced by FGF8 in the chick embryo. *Nature* **380,** 66-68.

Dattani, M. T., Martinez-Barbera, J. P., Thomas, P. Q., Brickman, J. M., Gupta, R., Martensson, I. L., Toresson, H., Fox, M., Wales, J. K., Hindmarsh, P. C., Krauss, S., Beddington, R. S. and Robinson, I. C. (1998). Mutations in the homeobox gene *HESX1/Hesx1* associated with septo-optic dysplasia in human and mouse. *Nat. Genet.* **19,** 125-133.

De Felice, M., Ovitt, C., Biffali, E., Rodriguez-Mallou, A., Arra, C., Anastassiadis, K., Macchia, V. and Di Lauro, R. (1998). A mouse model for hereditary thyroid dysgenesis and cleft palate. *Nat. Genet.* **19,** 395-398.

Dufort, D., Schwartz, L., Harpal, K. and Rossant, J. (1998). The transcription factor HNF3β is required in visceral endoderm for normal primitive streak morphogenesis. *Development* **125,** 3015-3025.

Dunwoodie, S. L., Rodriguez, T. A. and Beddington, R. S. (1998). *Msg1* and *Mrg1*, founding members of a gene family, show distinct patterns of gene expression during mouse embryogenesis. *Mech. Dev.* **72,** 27-40.

Echelard, Y., Epstein, D. J., St-Jacques, B., Shen, L., Mohler, J., McMahon, J. A. and McMahon, A. P. (1993). Sonic hedgehog, a member of a family of putative signaling molecules, is implicated in the regulation of CNS polarity. *Cell* **75,** 1417-1430.

Furuta, Y., Piston, D. W. and Hogan, B. L. (1997). Bone morphogenetic proteins (BMPs) as regulators of dorsal forebrain development. *Development* **124,** 2203-2212.

Hermesz, E., Mackem, S. and Mahon, K. A. (1996). *Rpx*: a novel anterior-restricted homeobox gene progressively activated in the prechordal plate, anterior neural plate and Rathke's pouch of the mouse embryo. *Development* **122,** 41-52.

Ho, C. Y., Houart., C, Wilson, S. W. and Stainier, D. Y. R. (1999). A role for the extraembryonic yolk syncytial layer in patterning the zebrafish embryo suggested by properties of the *hex* gene. *Curr. Biol.* **9,** 1131-1134.

Hogan, B., Beddington, R., Costantini, F. and Lacy, E. (1994). *Manipulating the Mouse Embryo. A Laboratory Manual.* New York, Cold Spring Harbor Laboratory Press.

Jones, C. M., Broadbent, J., Thomas, P. Q., Smith, J. C. and Beddington, R. S. (1999). An anterior signalling centre in *Xenopus* revealed by the homeobox gene *XHex*. *Curr. Biol.* **9,** 946-954.

Kaufman, M. H. (1992). *The Atlas of Mouse Development*. London, Academic Press.

Keng, V. W., Fujimori, K. E., Myint, Z., Tamamaki, N., Nojyo, Y. and Noguchi, T. (1998). Expression of *Hex* mRNA in early murine postimplantation embryo development. *FEBS Lett.* **426,** 183-186.

Kimura, S., Hara, Y., Pineau, T., Fernandez-Salguero, P., Fox, C. H., Ward, J. M. and Gonzalez, F. J. (1996). The *T/ebp* null mouse: thyroid-specific enhancer-binding protein is essential for the organogenesis of the thyroid, lung, ventral forebrain, and pituitary. *Genes Dev.* **10,** 60-69.

Kimura, S., Ward, J. M. and Minoo, P. (1999). Thyroid-specific enhancer-binding protein/thyroid transcription factor 1 is not required for the initial specification of the thyroid and lung primordia. *Biochimie* **81,** 321-327.

Lawson, K. A., Meneses, J. J. and Pedersen, R. A. (1991). Clonal analysis of epiblast fate during germ layer formation in the mouse embryo. *Development* **113,** 891-911.

Lazzaro, D., Price, M., de Felice, M. and Di Lauro, R. (1991). The transcription factor TTF-1 is expressed at the onset of thyroid and lung morphogenesis and in restricted regions of the foetal brain. *Development* **113,** 1093-104.

Liu, A., Losos, K. and Liu, A., Losos, K. and Joyner, A. L. (1999). FGF8 can activate *Gbx2* and transform regions of the rostral mouse brain into a hindbrain fate. *Development* **126,** 4827-4838.

Liu, P., Wakamiya, M., Shea, M. J., Albrecht, U., Behringer, R. R. and Bradley, A. (1999). Requirement for *Wnt3* in vertebrate axis formation. *Nat. Genet.* **22,** 361-365.

Macchia, P. E., Felice, M. D. and Lauro, R. D. (1999). Molecular genetics of congenital hypothyroidism. *Curr. Opin. Genet. Dev.* **9,** 289-294.

Martinez, S., Crossley, P. H., Cobos, I., Rubenstein, J. L. and Martin, G. R. (1999). FGF8 induces formation of an ectopic isthmic organizer and isthmocerebellar development via a repressive effect on *Otx2* expression. *Development* **126,** 1189-2000.

Meyers, E. N., Lewandoski, M. and Martin, G. R. (1998). An *Fgf8* mutant allelic series generated by Cre- and Flp-mediated recombination. *Nat. Genet.* **18**, 136-141.

Monaghan, A. P., Kaestner, K. H., Grau, E. and Schutz, G. (1993). Postimplantation expression patterns indicate a role for the mouse

forkhead/HNF-3α, β and γ genes in determination of the definitive endoderm, chordamesoderm and neuroectoderm. *Development* **119**, 567-578.

Mortensen, R. M., Conner, D. A., Chao, S., Geisterfer-Lowrance, A. A. and Seidman, J. G. (1992). Production of homozygous mutant ES cells with a single targeting construct. *Mol. Cell. Biol.* **12,** 2391-2395.

Newman, C. S., Chia, F. and Krieg, P. A. (1997). The *XHex* homeobox gene is expressed during development of the vascular endothelium: overexpression leads to an increase in vascular endothelial cell number. *Mech. Dev.* **66,** 83-93.

Nishina, H., Vaz, C., Billa, P., Nghiem, M., Sasaki, T., De la Pompa, J. L., Furlonger, K., Paige, C., Hui, C.-c., Fischer, K.-D., Kishimoto, H., Iwatsubo, H., Katada, T., Woodget, J. R. and Penninger, J. M. (1999). Defective liver formation and liver cell apoptosis in mice lacking the stress signaling kinase SEK1/MKK4. *Development* **126,** 505-516.

Oliver, G., Mailhos, A., Wehr, R., Copeland, N. G., Jenkins, N. A. and Gruss, P. (1995). *Six3*, a murine homologue of the sine oculis gene, demarcates the most anterior border of the developing neural plate and is expressed during eye development. *Development* **121,** 4045-4055.

Rhinn, M., Dierich, A., Shawlot, W., Behringer, R. R., Le Meur, M. and Ang, S. L. (1998). Sequential roles for *Otx2* in visceral endoderm and neuroectoderm for forebrain and midbrain induction and specification. *Development* **125,** 845-856.

Rubenstein, J. L., Shimamura, K., Martinez, S. and Puelles, L. (1998). Regionalization of the prosencephalic neural plate. *Annu. Rev. Neurosci.* **21,** 445-477.

Ruiz i Altaba, A., Prezioso, V. R., Darnell, J. E. and Jessell, T. M. (1993). Sequential expression of HNF-3β and HNF-3α by embryonic organizing centers: the dorsal lip/node, notochord and floor plate. *Mech. Dev.* **44,** 91-108.

Sasaki, H. and Hogan, B. L. (1993). Differential expression of multiple fork head related genes during gastrulation and axial pattern formation in the mouse embryo. *Development* **118,** 47-59.

Shalaby, F., Ho, J., Stanford, W. L., Fischer, K. D., Schuh, A. C., Schwartz, L., Bernstein, A. and Rossant, J. (1997). A requirement for *Flk1* in primitive and definitive hematopoiesis and vasculogenesis. *Cell* **89**, 981-990.

Shawlot, W. and Behringer, R. R. (1995). Requirement for *Lim1* in head-organizer function. *Nature* **374,** 425-430.

Shawlot, W., Deng, J. M. and Behringer, R. R. (1998). Expression of the mouse cerberus-related gene, *Cerr1*, suggests a role in anterior neural induction and somitogenesis. *Proc. Natl. Acad. Sci. USA* **95,** 6198-203.

Shawlot, W., Wakamiya, M., Kwan, K. M., Kania, A., Jessell, T. M. and Behringer, R. R. (1999). *Lim1* is required in both primitive streak-derived tissues and visceral endoderm for head formation in the mouse. *Development* **126,** 4925-4932.

Shimamura, K., Hartigan, D. J., Martinez, S., Puelles, L. and Rubenstein, J. L. (1995). Longitudinal organization of the anterior neural plate and neural tube. *Development* **121,** 3923-3933.

Shimamura, K. and Rubenstein, J. L. (1997). Inductive interactions direct early regionalization of the mouse forebrain. *Development* **124,** 2709-2718.

Spemann, H. and Mangold, H. (1924). Über induktion von embryonalanlagen durch implantation artfremder organisatoren. *Roux Arch. Entwick. Mech. Organ.* **100,** 599-638.

Tam, P. P. and Behringer, R. R. (1997). Mouse gastrulation: the formation of a mammalian body plan. *Mech. Dev.* **68,** 3-25.

Tam, P. P. and Steiner, K. A. (1999). Anterior patterning by synergistic activity of the early gastrula organizer and the anterior germ layer tissues of the mouse embryo. *Development* **126,** 5171-5179.

Tanaka, T., Inazu, T., Yamada, K., Myint, Z., Keng, V. W., Inoue, Y., Taniguchi, N. and Noguchi, T. (1999). cDNA cloning and expression of rat homeobox gene, *Hex*, and functional characterization of the protein. *Biochem. J.* **339,** 111-117.

Tao, W. and Lai, E. (1992). Telencephalon-restricted expression of BF-1, a new member of the HNF- 3/fork head gene family, in the developing rat brain. *Neuron* **8,** 957-966.

Thomas, P. and Beddington, R. (1996). Anterior primitive endoderm may be responsible for patterning the anterior neural plate in the mouse embryo. *Curr. Biol.* **6,** 1487-1496.

Thomas, P., Brickman, J., Pöpperl, H. Krumlauf, R. and Beddington, R. S. P. (1997). Axis duplication and anterior identity in the mouse embryo. *Cold Spring Harb. Symp. Quant. Biol.* **LXII,** 135-144.

Thomas, P. Q., Brown, A. and Beddington, R. S. (1998). *Hex*: a homeobox gene revealing peri-implantation asymmetry in the mouse embryo and an early transient marker of endothelial cell precursors. *Development* **125,** 85-94.

Varlet, I., Collignon, J. and Robertson, E. J. (1997). *nodal* expression in the primitive endoderm is required for specification of the anterior axis during mouse gastrulation. *Development* **124,** 1033-1044.

Walther, C. and Gruss, P. (1991). *Pax-6*, a murine paired box gene, is expressed in the developing CNS. *Development* **113,** 1435-1449.

Xuan, S., Baptista, C. A., Balas, G., Tao, W., Soares, V. C. and Lai, E. (1995). Winged helix transcription factor BF-1 is essential for the development of the cerebral hemispheres. *Neuron* **14,** 1141-1152.

Yamaguchi, T. P., Dumont, D. J., Conlon, R. A., Breitman, M. L. and Rossant, J. (1993). *flk-1*, an flt-related receptor tyrosine kinase is an early marker for endothelial cell precursors. *Development* **118,** 489-498.

Yatskievych, T. A., Pascoe, S. and Antin, P. B. (1999). Expression of the homebox gene *Hex* during early stages of chick embryo development. *Mech. Dev.* **80,** 107-9.

Ye, W., Shimamura, K., Rubenstein, J. L., Hynes, M. A. and Rosenthal, A. (1998). FGF and Shh signals control dopaminergic and serotonergic cell fate in the anterior neural plate. *Cell* **93,** 755-766.

Zambrowicz, B. P., Imamoto, A., Fiering, S., Herzenberg, L. A., Kerr, W. G. and Soriano, P. (1997). Disruption of overlapping transcripts in the ROSAβ *geo* 26 gene trap strain leads to widespread expression of β-galactosidase in mouse embryos and hematopoietic cells. *Proc. Natl. Acad. Sci. USA* **94,** 3789-3794.

Zannini, M., Avantaggiato, V., Biffali, E., Arnone, M. I., Sato, K., Pischetola, M., Taylor, B. A., Phillips, S. J., Simeone, A. and Di Lauro, R. (1997). TTF-2, a new forkhead protein, shows a temporal expression in the developing thyroid which is consistent with a role in controlling the onset of differentiation. *EMBO J.* **16,** 3185-97.

Zaret, K. (1998). Early liver differentiation: genetic potentiation and multilevel growth control. *Curr. Opin. Genet. Dev.* **8,** 526-531.

Zoltewicz, J. S., Plummer, N. W., Lin, M. I. and Peterson, A. S. (1999). *oto* is a homeotic locus with a role in anteroposterior development that is partially redundant with *lim1*. *Development* **126,** 5085-5095.